RESILIENT INFRASTRUCTURE
June 1–4, 2016
RESILIENT INFRASTRUCTURE LONDON 2016

MOMENT REDISTRIBUTION OF GFRP-RC CONTINUOUS T-BEAMS

S. M. Hasanur Rahman
M.Sc. Student, University of Manitoba, Canada

Ehab El-Salakawy
Professor and CRC in Durability and Modernization of Civil Structures, University of Manitoba, Canada

ABSTRACT

Fiber-reinforced polymer (FRP) bars have proven to be an excellent alternative to steel bars in many concrete structures such as parking garages and overpasses that are susceptible to harsh environments and consequently corrosion of steel reinforcement. In these structures, FRP reinforced concrete (FRP-RC) continuous beams are common members. Moment redistribution in FRP-RC continuous beams has not been well established yet because of the different characteristics of FRP bars such as linear-elastic stress-strain relationship and lower modulus of elasticity compared to conventional steel. Recent studies showed that redistribution of internal forces in Glass (G) FRP-RC continuous beams with a rectangular section is possible. However, no attention was given to continuous beams with a T-section. Therefore, this study aims at investigating the ability of GFRP-RC continuous beams with a T-section to redistribute the moment between the critical sections. In this paper, test results of three large-scale GFRP-RC T-beams are presented. The beams were 6,000-mm long and continuous over two equal spans of 2,800 mm each. The sections had an overall depth of 300 mm, an effective flange width of 600 mm, a flange thickness of 100 mm, and a web width of 200 mm. The test variables included the assumed moment redistribution percentage and the arrangement of shear reinforcement. It was observed that the beam with less stirrup spacing showed better performance in achieving the assumed percentage of moment redistribution and in carrying higher ultimate load compared to its counterparts with larger stirrup spacing.

Keywords: Moment Redistribution; T-section; Continuous beams; Fibre Reinforced Polymer (FRP).

1. INTRODUCTION

Fiber reinforced polymer (FRP) bars are being increasingly used in reinforced concrete (RC) structures, especially those in harsh weathering regions because of their effectiveness in avoiding deterioration of concrete caused by corrosion. FRP reinforced concrete (FRP-RC) continuous T-beam is one of the common structural elements in RC structures such as, parking garages, overpasses, and marine structures. For such type of beams, both the deformability and the moment redistribution are desirable and advantageous features that improve the overall performance and the utilization of full capacity of the sections along the beam. Since, FRP bars, unlike conventional steel, exhibit linear-elastic response of stress-strain relationship until failure; it raises the concern of deformability and consequently moment redistribution. However, several studies were conducted to investigate the moment redistribution of rectangular continuous beams. El-Mogy et al. (2010 and 2011) reported that approximately 23% moment redistribution was observed without any adverse effect on the beam performance. Also, closer spacing of stirrups, while maintaining the same transverse reinforcement ratio, was found to increase the moment redistribution. Mahmoud and El-Salakawy (2014 and 2016) also observed the moment redistribution in shear-critical GFRP-RC rectangular beams with different concrete strength, longitudinal reinforcement ratio and transverse reinforcement ratio. The authors also found that increasing stirrup diameter, while maintaining the same spacing, had little effect on moment redistribution. Moreover, Kara and Ashour (2013) developed a numerical technique, and studied moment-curvature and moment redistribution. The authors concluded that under-reinforced FRP-RC beams could not redistribute bending moment and that the critical sections, once reached their capacity, were not able to redistribute bending moments.

However, in addition to the fact of linearity of stress-strain response of FRP bars, T-shaped section in continuous beams draws further research attention because of interaction between the mid-span with higher stiffness and the middle support region with comparatively lower stiffness at the post-cracking stage. Scholz (1993) explored the significant effect of variation of stiffness on neutral axis-to-depth ratio and thus, moment redistribution in steel-RC continuous beams. In contrast to the stiffness variation, the mid-span region, at the pre-cracking stage, has lower section modulus while the region over middle support has higher section modulus. Also, the neutral axis-to-depth ratio at mid-span being lower than that of middle support region counteracts the influence of stiffer mid-span in redistributing moments. Santos et al. (2013) tested seven small-scale GFRP-RC T-beams to study the effect of reinforcement ratio and confinement on the moment redistribution. The authors concluded that higher reinforcement ratio at mid-span, and higher confinement at middle support zone increased the moment redistribution. In this study, the possibility and the extent of moment redistribution of large-scale continuous concrete beams with T-section are investigated.

2. EXPERIMENTAL PROGRAM

2.1 Test Specimens

Three large-scale continuous beams with T-section were constructed and tested to failure. The test beams were 6,000 mm long and continuous over two equal spans of 2,800 mm each. All beams were reinforced with GFRP bars and stirrups. The test parameters included the assumed percentage of moment redistribution and the arrangement of shear reinforcement. Figure 1 shows the dimensions, reinforcement arrangement, and internal instrumentation of the tested beams.

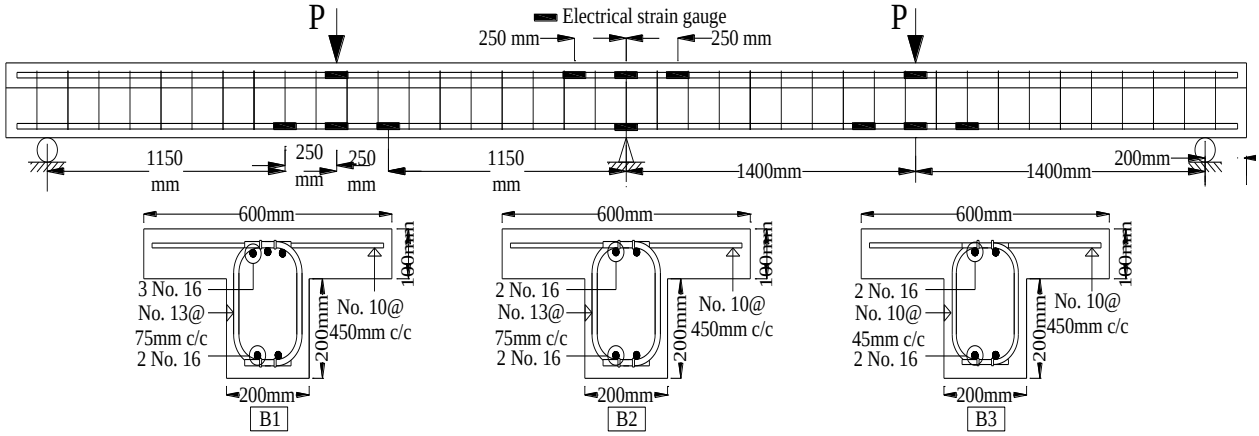

Figure 1: Dimensions, details of reinforcement and internal instrumentation of test beams.

The information reported in this paper is part of an ongoing research project in which a steel-RC control beam was constructed to carry a design load of 155 kN. Accordingly, GFRP-RC beam B1 was designed following the Canadian standard CSA/S806-12 (CSA 2012) to meet that design load without any moment redistribution. Then, both beam B2 and B3 were provided with longitudinal reinforcements to satisfy an assumed percentage of moment redistribution of 15% from the middle support to the mid-span section of each beam.

Table 1: Reinforcement Details of Tested Beams

Beam	Longitudinal reinforcement				Transverse reinforcement	
	Top bars over middle-support		Bottom bars at mid-span		Stirrup diameter (mm)	Spacing (mm)
	Bars	ρ/ρ_b	Bars	ρ/ρ_b		
B1	3 No. 16	4.73	2 No. 16	1.05	No. 13	75
B2	2 No. 16	3.27	2 No. 16	1.10	No. 13	75
B3	2 No. 16	3.10	2 No. 16	1.04	No. 10	45

In all beams, both the hogging and the sagging moment regions were over-reinforced (ratio (ρ/ρ_b) with reinforcement ratio provided, ρ to balanced reinforcement ratio, ρ_b of more than 1, as given in Table 1) to have favourable compression-controlled failure. However, the required transverse reinforcement (stirrups) was achieved by using 13 mm-diameter stirrup with spacing of 75 mm in beam B1 and B2. Also, based on previous studies (El-Mogy et al. 2011, Mahmoud and El-Salakawy 2016), it was concluded that using smaller diameter-stirrup rather larger diameter-stirrup, while maintaining the same shear reinforcement ratio, has pronounced effect on moment redistribution. As such, 10 mm-diameter stirrups with spacing of 45 mm, while maintaining almost same ratio of transverse reinforcement, were chosen for beam B3 to study the effect of stirrup-spacing. The spacing of stirrups was maintained within the minimum spacing requirements as required by CSA/S806-12 standard (1.4 times the longitudinal reinforcement diameter, 1.4 times the maximum aggregate size, or 30 mm). The beam flange was reinforced with No. 10 to satisfy the requirement of minimum reinforcement in the transverse direction.

2.2 Material Properties

Normal weight, ready-mixed concrete with a target 28-day compressive strength of 40 MPa was used to cast all beams. Maximum size of aggregate used in concrete mix was 20 mm. On the day of testing, at least five cylinders of standard size (100 mm × 200 mm) were tested to determine the average concrete compressive strength. The average compressive strength of beams B1, B2 and B3 were 44, 42, and 45 MPa, respectively.

Sand-coated GFRP bars were used as longitudinal and transverse reinforcement. The characteristic design values, according to CSA/S806-12 (CSA 2012), were determined from the material certificate received from the manufacturer. The mechanical properties of the reinforcement are summarized in Table 2.

Table 2: Properties of Reinforcing Materials

Material type	Bar designation	Diameter (mm)	Tensile strength (MPa)	Elastic modulus (GPa)	Strain (%)
GFRP	No. 10	9.5	1,770	65	2.7
	No.10 (bent)	9.5	1,350[a]	52[a]	2.6[a]
	No.13 (bent)	12.7	1,330[a]	53[a]	2.5[a]
	No.16	15.9	1,680	65	2.6

Note: [a] Straight portion property.

Three load cells were used at supports to measure the reactions during the test. Also, linear variable displacement transducers (LVDTs) were placed at quarters and mid-point of both spans (Fig. 2) to measure deflection. Moreover, PI-gauges were attached to record the crack width at critical sections; one at middle support and one at each mid-span. The internal instrumentation consisted of nine electrical strain gauges (Fig. 1) attached to the longitudinal reinforcement, and three concrete strain gauges attached to the extreme compression side of concrete.

A 1000-kN MTS hydraulic machine was used to apply concentrated load on a stiff steel spreader beam that, in turn, delivered the load to the mid-point of both spans. The applied load on each span was then evenly transferred to the beam through another spreader beam that was placed across the beam flange. Loading was applied at a rate of 10 kN/min and equal load on both spans was maintained throughout the test. Readings of all instrumentations were acquired and stored using a data acquisition (DAQ) system.

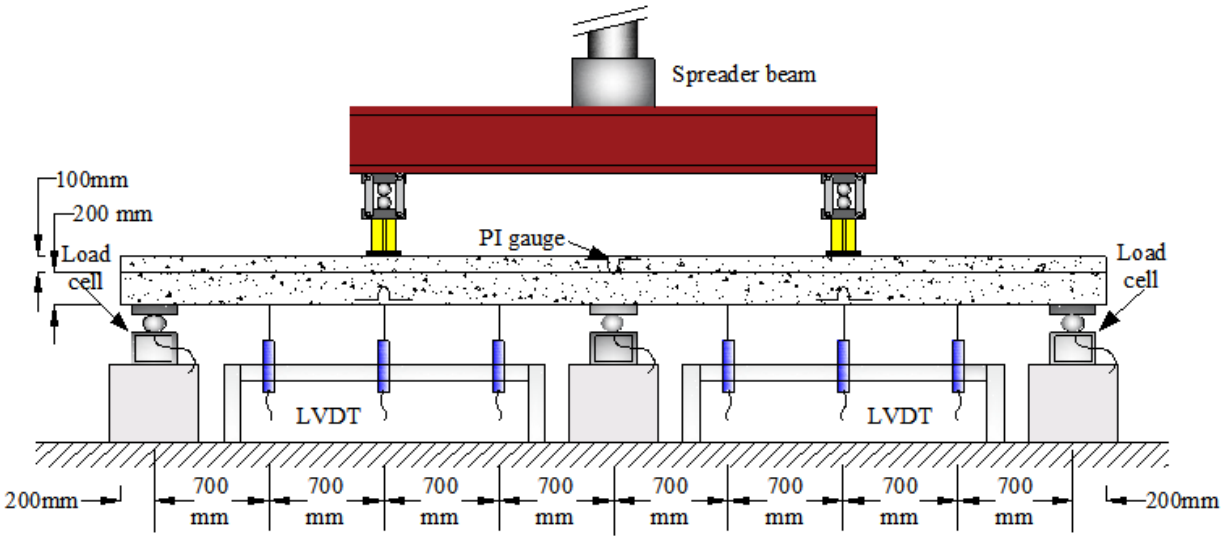

Figure 2: Experimental set up for test specimens.

3. TEST RESULTS

3.1 Cracking Behaviour and Mode of Failure

All beams showed similar cracking behaviour until failure. The first flexural crack in all beams formed in the sagging moment region in both spans followed by vertical flexural crack over the middle support. The cracking load at sagging region of all beams ranged between 19 and 25 kN, while that at hogging region varied from 35 to 38 kN. This behaviour was observed because of lower section modulus of the sagging moment region compared to that of the hogging moment region. The majority of flexural cracks initiated at a load up to 50-60% of failure load and those, once initiated, propagated towards the compression zone as loading was continuing. Approaching failure, few diagonal tension cracks developed in the interior shear span. Also, it was noted that the hogging moment regions in all beams had small number of wider cracks in contrast to large number of narrower cracks in sagging moment region. In addition, there was a longitudinal crack observed along each flange-web interface of both spans in all beams. Due to such longitudinal cracking, the composite behaviour of T-section at mid-span was significantly reduced and the beam moved towards the behaviour of a rectangular section.

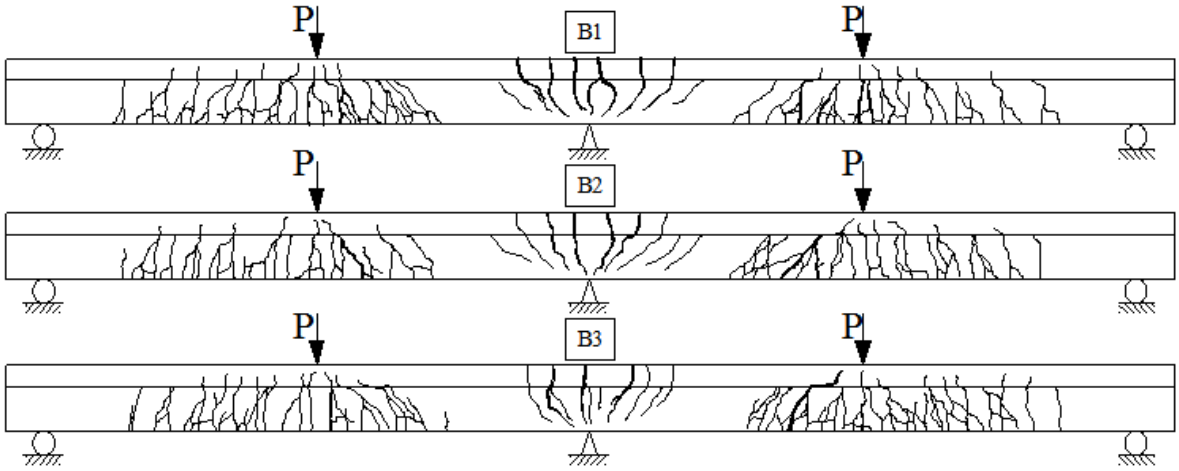

Figure 3: Cracking pattern of tested beams

In all beams, concrete crushing initiated at hogging moment region (spalling of concrete can be seen in Fig. 4) before the beams reached failure by concrete crushing at sagging moment region. This was evident since the concrete strains

at middle support section reached the ultimate crushing strain as described in the next section, while the strains in longitudinal bars (Fig. 5) were well below the characteristic design values.

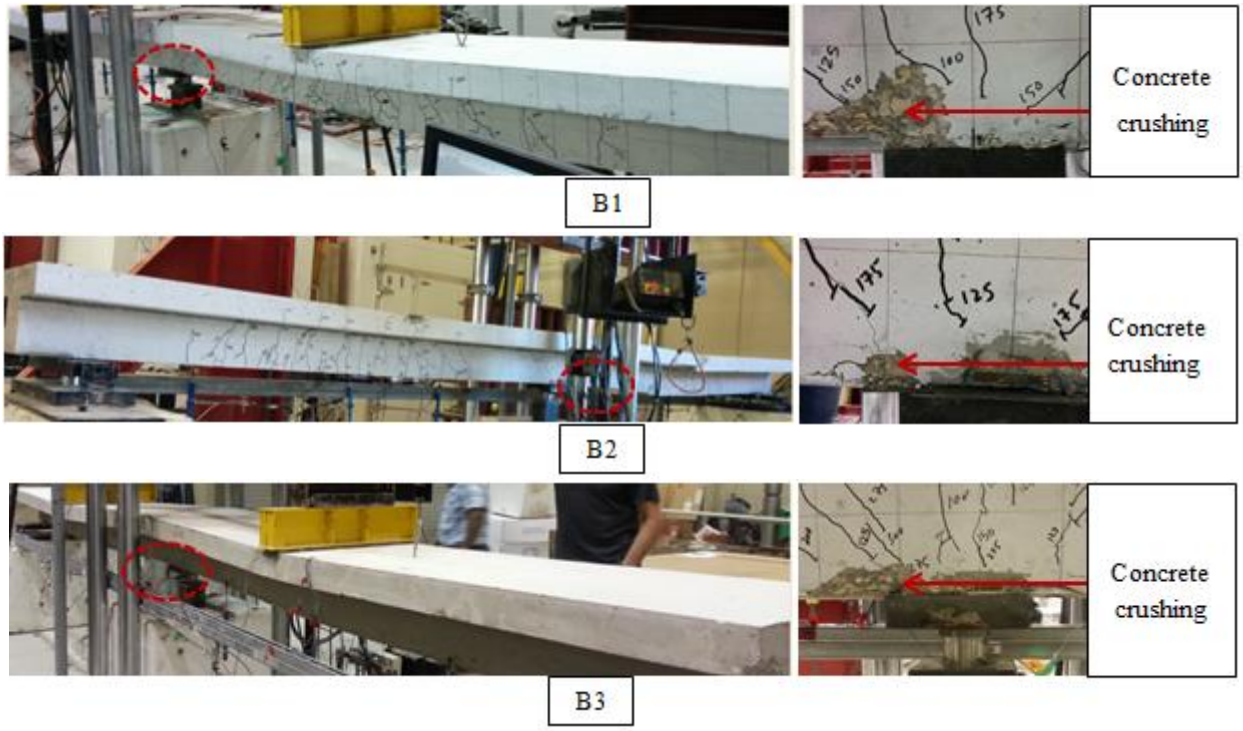

Figure 4: Failure mode of tested beams

3.2 Strain in Reinforcement and Concrete

The load-strain relationship for both concrete and longitudinal reinforcement at the hogging and the sagging moment regions are plotted in Fig. 5. The strain values in concrete over middle support were higher than or very close to the crushing strain, 3,500 micro-strains, specified in the CSA-S806-12. On the other hand, after the cracks took place along the interface of web and flange in the sagging moment region, the flange substantially got relieved from resisting the applied load, which is indicated by the lower measured strain in the concrete at the mid-span section.

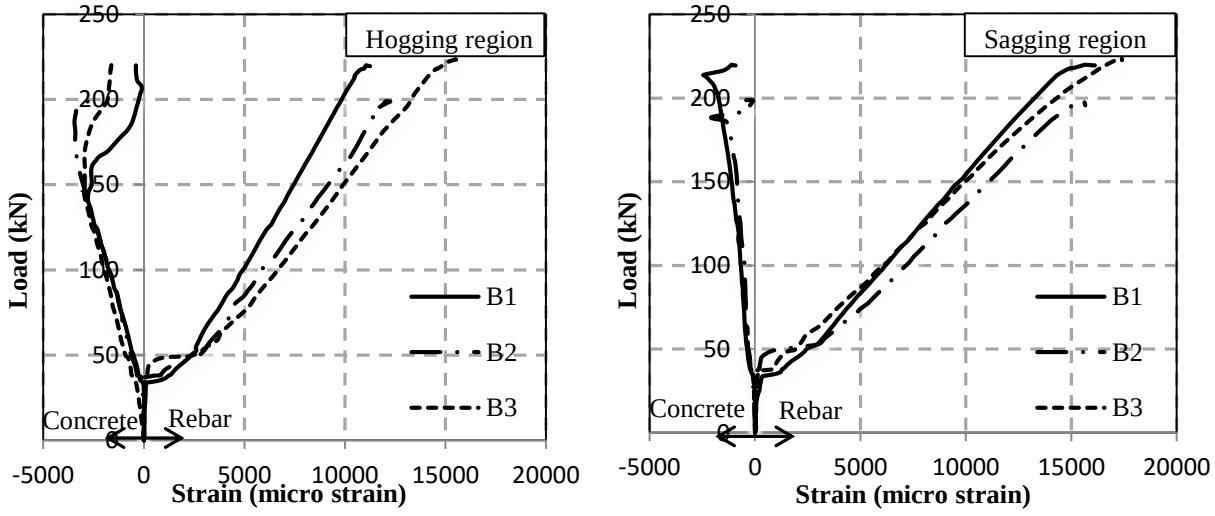

Figure 5: Variation of strain in GFRP bars with load

It is also worth mentioning that all beams, after concrete strains reached the maximum at middle support section, continued to resist more loads until failure took place at mid-span. In contrast to concrete strains, the strain values in reinforcing bars at mid-span sections, especially at higher stage of loading, were higher than that at middle support sections in all beams. This was due to the lower amount of longitudinal reinforcement in mid-span section of beam B1 whereas, in case of beam B2 and B3, higher moment due to redistribution resulted in higher strains.

3.3 Load-Deflection Response

For each beam, maximum deflections measured at both spans were very similar. Therefore, the average of both span deflections was reported for each test beam. As mentioned earlier, cracks first formed in the sagging moment regions followed by cracking in the hogging moment region. However, it can be seen that, in load-deflection behaviour demonstrated in Fig. 6, cracking at mid-span had little effect on increasing deflection at early stage of loading. Significant change in the flexural stiffness of the beams took place once cracks formed over the middle support that resulted in increasing the mid-span deflection rapidly. Overall, load-deflection behaviour of all beams in post-cracking stage was approximately linear until signs of concrete spalling were observed. Afterwards, some nonlinearity of load-deflection relationship was noted near failure, which can be attributed to the nonlinearity of concrete at middle support region and the formation of diagonal cracks within the span.

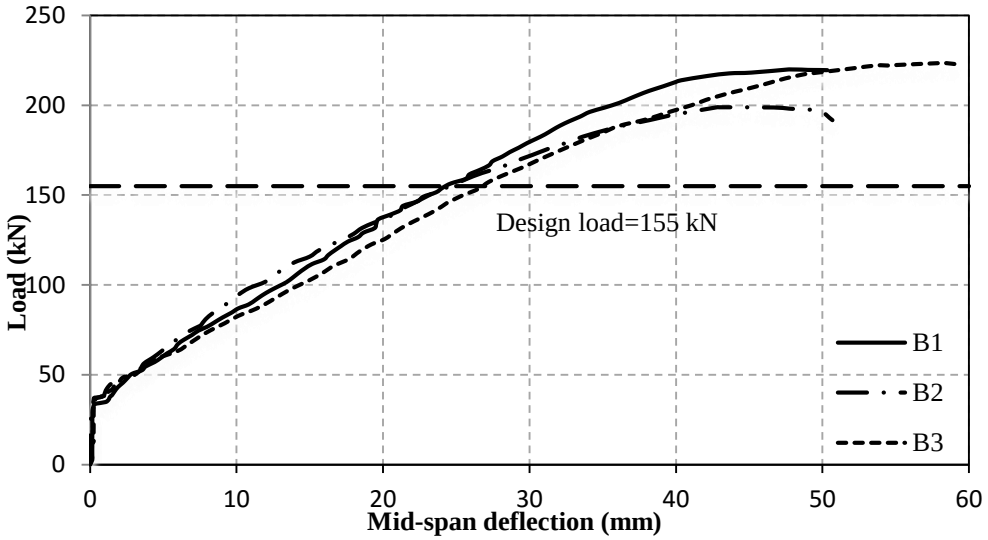

Figure 6: Load-deflection behaviour of tested beams

All beams not only reached the target design load of 155 kN (Fig. 6) but also carried additional load of 28-43% the design load. The deflections of all beams, measured at design load level, were similar, while at failure load, the deflection of beam B3 was slightly higher compared to both B1 and B2. However, a little stiffer response of beam B1 stemmed from lower strain of reinforcing bars (Fig. 5) because of higher reinforcement ratio over middle support. It can also be noted in Fig. 6 that beam B3, in comparison to its counterpart B2, not only carried 12% more load but also experienced 17% more deflection before failure. This superior performance could be possible due to the smaller spacing of stirrups (45 mm) in beam B3 compared to larger spacing of stirrups (75 mm) in beam B2.

3.4 Moment Redistribution

Formation of cracks in the sagging moment region before the hogging moment region slightly reduced the flexural stiffness of the sagging moment region and thus, reversed insignificant amount of load towards the middle support. However, cracking of the hogging moment region caused the section to rotate substantially over middle support, and resulted in load redistribution from hogging region to sagging region. The end reactions against the applied load on each span (P) of all beams were plotted in Fig. 7, and compared with the elastic end reaction of $0.3125P$. The experimental end reactions of all beams in the post-cracking stage were higher than that calculated based on elastic theory. This finding obviously showed that the load, especially in beam B2 and B3, significantly redistributed from hogging to sagging region.

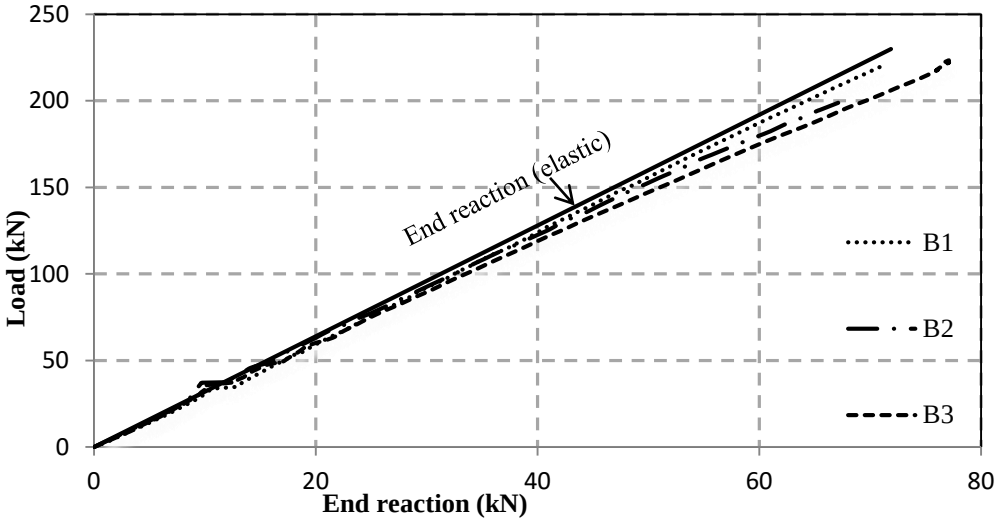

Figure 7: Comparison of end reactions of tested beams

The failure loads along with the experimental and the theoretical moments are also shown in Fig. 8. Beam B1, designed for no moment redistribution, redistributed 4.8% moment at design load (155 kN) level and was able to reach 5.7% at failure load. Beam B2, at design load, could achieve 8.1% moment redistribution; however, at failure load, the beam exhibited 14.8% moment redistribution which is slightly less than the assumed value. On the other hand, beam B3 could successfully attain the target percentage of moment redistribution even at design load. The percentage of moment redistribution, achieved by beam B3, was 15.2 and 17.4% at design load and failure load, respectively. This better performance of beam B3 in redistributing moments can be attributed to rotational capability that was enhanced by confinement provided by the stirrups with smaller spacing.

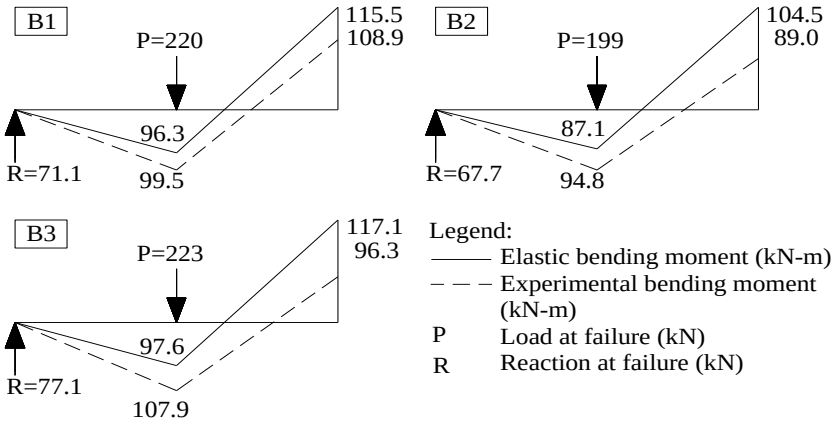

Figure 8: Moment redistribution of tested beams

4. CONCLUSIONS

Based on the test results discussed in this paper, the following conclusions can be drawn:

1. All tested beams experienced compression-controlled failure and were able to carry further load even after concrete spalling was noticed at the hogging moment region. The smaller stirrup spacing enabled beam B3 to carry more load as well as to undergo more deflection compared to its counterpart with larger stirrup spacing.
2. The longitudinal crack developed at the web-flange interface in mid-span region caused the failure of the beams before reaching their full capacity as T-section.

3. All beams exhibited moment redistribution from hogging to sagging moment region. Beam B1 designed for elastic moments reached 5.7% moment redistribution before it failed. Beam B2 and B3 could successfully meet the target redistribution of moments that they were designed for. Beam B2 achieved 14.8% moment redistribution while beam B3 demonstrated maximum 17.4% before failure.

ACKNOWLEDGEMENTS

The authors are expressing their gratitude and sincere appreciation for the financial support received from Natural Science and Engineering Research Council of Canada (NSERC), through Canada Research Chairs program. Also, the authors are acknowledging the help received from the technical staff of McQuade Heavy Structures Laboratory of University of Manitoba.

REFEENCES

Canadian Standard Association (CSA), 2012. Design and Construction of Building Structures with Fibre-Reinforced Polymers. *CAN/CSA-S806-12*, Rexdale, Ontario. Canada.

Canadian Standard Association (CSA). 2006. Canadian Highway Bridge Design Code, *CAN/CSA-S6-06*, Rexdale, Ontario. Canada.

El-Mogy, M., El-Ragaby, A., and El-Salakawy, E. 2010. Flexural Behavior of Continuous FRP-Reinforced Concrete Beams. *Journal of Composites for Construction*, Vol. 14, No. 6, pp. 669–680.

El-Mogy, M., El-Ragaby, A. and El-Salakawy, E. (2011), "Effect of Transverse Reinforcement on the Flexural Behavior of Continuous Concrete Beams Reinforced with FRP", *Journal of Composites for Construction*, Vol. 15, No. 5, pp. 672-681.

Kara, I. F. and Ashour, A. F. 2013. Moment Redistribution in Continuous FRP Reinforced Concrete Beams. *Construction and Building Materials*, Vol. 49, pp. 939-948.

Mahmoud, K. and El-Salakawy, E. 2014. Shear Strength of GFRP-Reinforced Concrete Continuous Beams with Minimum Transverse Reinforcement. *Journal of Composite for Construction*, 18 (1), 04013018, DOI: 10.1061/(ASCE)CC.1943-5614.0000406..

Mahmoud, K. and El-Salakawy, E. 2016. Effect of Transverse Reinforcement Ratio on the Shear Strength of GFRP-RC Continuous Beams. *Journal of Composite for Construction*, 20 (1): 04015023, DOI: 10.1061/(ASCE)CC.1943-5614.0000583.

Santos, P., Laranja, G., Franca, P. M. and Correia, J. R. 2013. Ductility and Moment Redistribution Capacity of Multi-Span T-Section Concrete Beams Reinforced with GFRP Bars. *Construction and Building Materials*, Vol. 49, pp. 949–961.

Scholz, H. 1993. Contribution to Redistribution of Moments in Continuous Reinforced Concrete Beams. *ACI Structural Journal*, V 90, No. 2.